Tamara Wirth*, Ady Naber, and Werner Nahm

Combination of Color and Focus Segmentation for Medical Images with Low Depth-of-Field

Abstract: Image segmentation plays an increasingly important role in image processing. It allows for various applications including the analysis of an image for automatic image understanding and the integration of complementary data. During vascular surgeries, the blood flow in the vessels has to be checked constantly, which could be facilitated by a segmentation of the affected vessels. The segmentation of medical images is still done manually, which depends on the surgeon's experience and is time-consuming. As a result, there is a growing need for automatic image segmentation methods. We propose an unsupervised method to detect the regions of no interest (RONI) in intraoperative images with low depth-of-field (DOF). The proposed method is divided into three steps. First, a color segmentation using a clustering algorithm is performed. In a second step, we assume that the regions of interest (ROI) are in focus whereas the RONI are unfocused. This allows us to segment the image using an edge-based focus measure. Finally, we combine the focused edges with the color RONI to determine the final segmentation result. When tested on different intraoperative images of aneurysm clipping surgeries, the algorithm is able to segment most of the RONI not belonging to the pulsating vessel of interest. Surgical instruments like the metallic clips can also be excluded. Although the image data for the validation of the proposed method is limited to one intraoperative video, a proof of concept is demonstrated.

Keywords: image segmentation, regions of no interest, low depth-of-field (DOF), edge linking.

https://doi.org/10.1515/cdbme-2018-0083

1 Introduction

The application of medical imaging techniques is expanding with increasing digitalization, but accurate segmentation of medical images remains a challenge. In vascular surgeries, the segmentation of the affected vessels could support the surgeons in the essential task of surveilling and securing the blood flow. As current segmentation methods can only be applied to specific images, medical image segmentation is still done manually by experts or clinicians. Although manual segmentation is accurate, it is time-consuming and tedious. [1] For this reason, unsupervised methods for medical image segmentation are needed.

Nowadays, image segmentation based on color features is frequently used in medical applications [2]. In intraoperative images however, color information is not sufficient to detect the regions of interest (ROI). In case of an image with low depth-of-field (DOF), a focus-based segmentation can be applied. Tsai and Wang used an edge-based method that determines the amount of defocus of edge pixels [3]. An example of a region-based approach is presented in Wang et al., where the high frequency components are detected using wavelet coefficients [4]. Recently, Lo and Chang proposed to combine a region-based defocus map with superpixel grouping and its edge and color similarity attributes to detect the focused foreground of the image [5]. These methods however are not designed to segment an image of a surgical scene. In this paper, we propose a method that combines color and focus segmentation to detect the regions of no interest (RONI) in medical images with low DOF. We work on medical images of invasive surgeries displaying a surgical working channel, which induces a low DOF due to the high magnification of the recording system.

2 Methods

The proposed method is divided into three parts (see figure 1). A color segmentation is performed on the original image and focused edges are detected. Finally, the outputs of the previous two steps are combined to obtain the final segmentation result.

***Corresponding author: Tamara Wirth:** Karlsruhe Institute of Technology (KIT), Institute of Biomedical Engineering (IBT), Kaiserstrasse 12 in 76135 Karlsruhe, Germany, e-mail: publications@ibt.kit.edu

Ady Naber, Werner Nahm: Karlsruhe Institute of Technology (KIT), Institute of Biomedical Engineering (IBT), Karlsruhe, Germany

All processing was done in MATLAB R2017b.

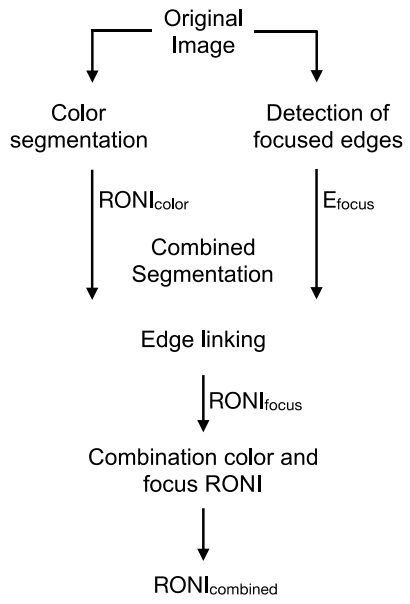

Figure 1: The flow diagram of the proposed segmentation method.

2.1 Image data

The images used to evaluate the algorithm are single frames taken from a publicly available video on the Carl Zeiss Meditec AG website [6]. The RGB images have a resolution of 560x470 pixels and show an aneurysm before and after clipping. Due to the high magnification and the depth of the working channel, the images possess a low depth of field. The vessel of interest is assumed to be completely exposed and to lie in the focus plane of the capturing camera.

2.2 Color segmentation

The goal of the color segmentation is to detect the pixels that do not have the color of human tissue and thus belong to the RONI. This includes unlit black regions, white light reflections and surgical tools, which usually are gray colored. We first convert the RGB pixel values to CIELAB space. Subsequently, the k-means clustering algorithm is applied to segment the pixels into three coherent color regions.

To increase the probability of convergence to a global minimum, we repeat the clustering algorithm five times and choose the result with the lowest within-cluster variance. The corresponding $RONI_{color}$ is then identified as the cluster possessing the smallest mean distance to achromatic grayscale values, which are located on the lightness axis (L) in the CIELAB color space.

2.3 Detection of focused edges

We use an edge-based focus measure proposed by Tsai and Wang to calculate a focus map from the original image [3].

First of all, the original image $I(x,y)$ is converted to a grayscale image from which the gradient image $g(x,y)$ is calculated using the Sobel edge operator. The amount of defocus of an edge pixel is defined as the proportion of edge pixels p_e in a neighborhood window $N(x,y)$ using the moment-preserving method.

$$\boldsymbol{p_e} = \frac{\boldsymbol{number\ of\ edge\ pixels\ in\ N(x,y)}}{\boldsymbol{total\ number\ of\ pixels\ in\ N(x,y)}} \tag{1}$$

The more an edge is out of focus, the more it is blurred, which results in a larger value of p_e. With $p_e \in (0,1]$, focused edge pixels result in p_e close to zero, whereas p 1 indicates no edge at all. As this focus measure is only defined for edge pixels, the value for all other pixels is set 1.

The algorithm to measure the amount of edge focus does not differentiate between two focused edges and one defocused edge in $N(x,y)$. For this reason, the size of the neighborhood window should be small enough to only contain one single edge, but still large enough to estimate p reliably. We choose a square neighborhood window N of size 7x7 pixels. The focused edges can be detected by applying a threshold $T_e = 0.5$ to the resulting p_e focus map.

2.4 Combined segmentation

In this step, the focused edges detected in the previous step are combined with the $RONI_{color}$ to obtain the final segmentation result.

2.4.1 Edge linking

To obtain an enclosed $RONI_{focus}$, the detected focused edges are linked using a combination of morphological operations and Canny edge detection. Before linking the focused edges , all edges that belong to the color RONI are excluded.

(2)

Then, the Canny edge operator is applied to the original image and the superposition of Canny edges E_{canny} and is kept to narrow down the edge width to one pixel. [7]

(3)

To link the focused edges, first all Canny edge segments superposing with a focused edge are added. This is done by

morphological reconstruction, which describes the repeated dilation of $E_{focusThinned}$ without exceeding E_{canny}.

Those segments of the connecting Canny edges added in the previous step that do not connect two focused edge segments are then removed. These are identified as segments possessing less than three connections to $E_{focusThinned}$ and more than two open endpoints.

After that, gaps up to six pixels between open endpoints and E_{focus} are closed. Finally, the endpoints of the edges up to 40 pixels apart are linked to each other to obtain an enclosed region. The closest connection from an endpoint to another open endpoint or a focused edge $E_{focusThinned}$ is determined using a geodesic distance map.

2.4.2 Combination of color and focus RONI

The largest area enclosed by focused edges is defined as the ROI, all other regions belong to the $RONI_{focus}$. This result is now connected with the $RONI_{color}$ by a logical OR function.

$$\boldsymbol{RONI_{combined} = RONI_{color} \cup RONI_{focus}} \quad (4)$$

2.5 Evaluation

To evaluate the segmentation algorithm, the results will be compared to the ground truth, which is obtained by manual segmentation. The ground truth $RONI_{GT}$ includes unlit areas, light reflexes, surgical instruments and all tissues except the vessel of interest. The evaluation is done by calculating the Jaccard index as measure of similarity, the sensitivity and the specificity with respect to the ground truth.

3 Results

The segmentation results of the proposed algorithm are demonstrated on two intraoperative test images. Figure 2 shows an aneurysm before clipping, figure 4 after it has been clipped. Figures 3 and 5 show the corresponding segmentation results in which the identified $RONI_{combined}$ using color and focus parameters are blackened. The results of the evaluation are represented in table 1 and table 2 for the images of the aneurysm before and after clipping respectively. For comparison, the Jaccard index, sensitivity and specificity were also calculated for the results obtained by color and focus segmentation only.

Table 1: Evaluation of the segmentation result for the first aneurysm (figure 4). Comparison between color, focus segmentation and the combination of the two segmentations.

Evaluation method	Color segmentation	Focus segmentation	Combined segmentation
Jaccard index	0.4932	0.8733	0.9201
Sensitivity	0.4951	0.8769	0.9250
Specificity	0.9787	0.9766	0.9698

Table 2: Evaluation of the segmentation result for the second aneurysm (figure 5). Comparison between color, focus segmentation and the combination of the two segmentations.

Evaluation method	Color segmentation	Focus segmentation	Combined segmentation
Jaccard index	0.6428	0.7145	0.8862
Sensitivity	0.6484	0.7248	0.9053
Specificity	0.9154	0.8589	0.7901

4 Discussion

The segmentation result in figure 3 shows good accuracy in detecting the $RONI_{GT}$. From visual evaluation, the ROI_{GT} has not been reduced, which is reflected by a specificity of 0.9698. The sensitivity of 0.9250 shows that the algorithm fails to detect only few $RONI_{GT}$, which are in focus and lie in the same color range as the vessel of interest. White reflexes on the aneurysm that lead to saturation of the camera sensor can be removed as well as the black and gray regions on the upper right of the aneurysm. In figure 5, the region on the upper left of the aneurysm that is not correctly identified as RONI. It is a focused tissue-colored region similar to the false negative regions in figure 3. The metallic clip and the white swab in the upper right part of the image are excluded. In this image, the lower part of the aneurysm is out of focus and is thus falsely detected as RONI. This results in a lower specificity and Jaccard index than for the result in figure 3. In both images, the color components black, white and gray, which have been defined as RONI are segmented correctly. Additionally, the working channel is no longer visible after segmentation, which indicates a successful focus segmentation.

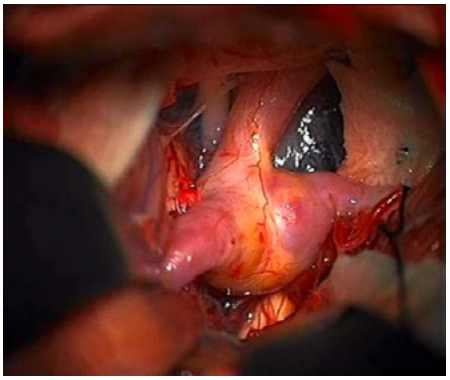

Figure 2: RGB image of the aneurysm before clipping.

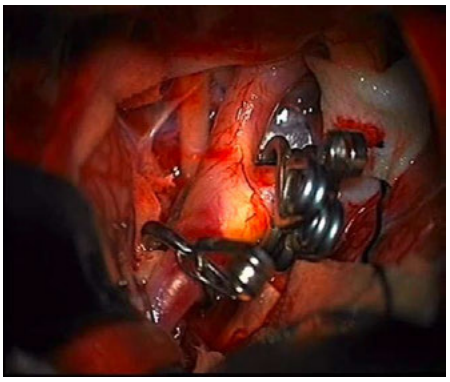

Figure 3: RGB image of the aneurysm after clipping.

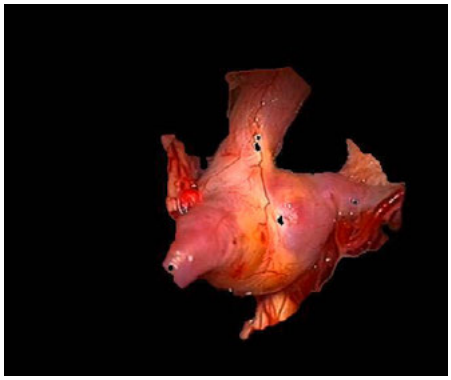

Figure 4: Segmentation result of the aneurysm before clipping.

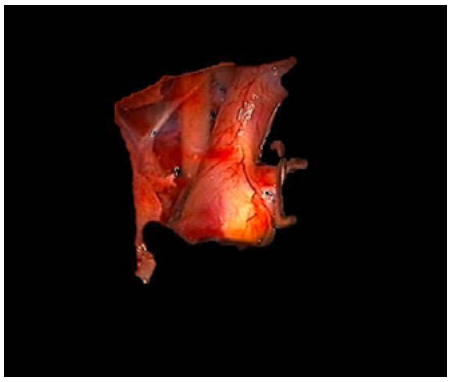

Figure 5: Segmentation result of the aneurysm after clipping.

Compared to only color or focus segmentation, the combined segmentation produces higher values for the Jaccard index and sensitivity. Only the specificity decreases, which was expected due to the trade-off between sensitivity and specificity. However, the algorithm is limited in segmenting tissue-colored focused RONI and unfocused ROI. Furthermore, with an edge-based focus measure, focused regions not containing any edges are difficult to identify.

5 Conclusion

The segmentation of intraoperative images is an important step in assisting the surgeon by enhancing the display of the surgical scene. We proposed an unsupervised image segmentation algorithm to detect the RONI in medical images with low DOF. The algorithm combines the segmentation based on color and focus parameters. This work shows a proof of concept as well as the limitations of the proposed method. So far, statistical evaluation was done on two intraoperative images. With the access to more test images, a more profound evaluation of our segmentation algorithm will be possible. In future work, the focus segmentation can be performed using different focus measures and the combined segmentation results can be compared to the current results.

Author's Statement

Research funding: Mr. Ady Naber receives a scholarship of the Karlsruhe School of Optics & Photonics. Conflict of interest: Authors state no conflict of interest. Informed consent: Informed consent has been obtained from all individuals included in this study. Ethical approval: The research related to human use complies with all the relevant national regulations, institutional policies and was performed in accordance with the tenets of the Helsinki Declaration, and has been approved by the authors' institutional review board or equivalent committee.

References

[1] Zou W, Xie Y. Interactive Medical Image Segmentation Using Snake and Multiscale Curve Editing. In: Computation and Mathematical Methods in Medicine 2013; 2013:1-13.

[2] Hance GA, Umbaugh RH, Moss RH, Stoecker WV. Unsupervised color image segmentation with application to skin tumor borders. In: IEEE Engineering in Medicine and Biology 1996; 15(1):104-111.

[3] Tsai DM, Wang HJ. Segmenting focused objects in complex visual images. In: Pattern Recognit. Lett. 1998; 19:929-949.

[4] Wang JZ, Li J, Gray RM, Wiederhold G. Unsupervised Multiresolution Segmentation for Images with Low Depth of Field. In: IEEE Trans. Pattern Anal. Mach. Intell. 2001; 23(1):85-90.

[5] Lo CK, Chang LW. Unsupervised Image Segmentation using Defocus Map and Superpixel Grouping. In: Fifteenth IAPR International Conf. on Mach. Vision Appl. (MVA). 2017.

[6] www.zeiss.de/meditec/produkte/neurochirurgie/intraoperative-fluoreszenz/vaskular/infrared-800.html [03/13/2018], recorded by Volker Seifert, Frankfurt, Germany, 2006.

[7] Canny J. A Computational Approach to Edge Detection. In: IEEE Trans. Pattern Anal. Mach. Intell. 1986; 8(6):679-698.